

Charge transfer in proton-hydrogen-molecule collisions

Pritam P. Ray

Department of Physics, Visva-Bharati University, Santiniketan, W. B. 731 235, India

B. C. Saha

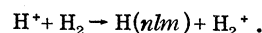
Department of Theoretical Physics, Indian Association for the Cultivation of Science, Calcutta 700 032, India

(Received 21 August 1979; revised manuscript received 19 May 1980)

Charge transfer into a number of excited s states of atomic hydrogen by proton impact on hydrogen molecule has been studied for both gerade and ungerade transitions of the molecular ion for the energy range 50 keV to 5 MeV. Using a contour integral representation of the hydrogenic wave function, the molecular Brinkman-Kramers amplitude has been expressed in a closed form, while the molecular Jackson-Schiff amplitude involving proton-proton interactions has been reduced to a one-dimensional integral over the real variables. Just as in the case of ground-state formation of hydrogen atoms, molecular effects play a significant role in the case of excited-state capture of an electron; and a hydrogen molecule cannot be regarded as a pair of independent hydrogen atoms at any energy in the considered range. The cross sections at a particular energy satisfy the inverse n^3 law approximately. The charge transfer involving the gerade transition of the molecular ion is the most important process; although, depending on the choice of the molecular wave function, there is a 10–28 % chance of the charge-transfer process involving the ungerade transition.

I. INTRODUCTION

The study of charge-exchange processes is important in understanding various physical phenomena occurring in planetary atmospheres, in interstellar medium and in plasma devices. This has gained further impetus for its role in the production of high Rydberg states of atoms. Because of its simplicity, charge-transfer studies for proton-hydrogen-atom collision continues to draw attention of theoretical physicists.¹ It is difficult, however, to measure these cross sections in atomized gases and as such there has been a number of experiments² on the charge transfer in proton-hydrogen-molecule collisions. For comparing theory with experiment, it has been customary to assume that a hydrogen molecule behaves like a pair of independent atoms. Naturally, the question arises as to whether it is justified to regard a hydrogen molecule as two independent hydrogen atoms. To resolve this question Wittkower *et al.*³ performed an experiment and showed that the molecular charge-exchange cross section σ_M is (2.40 ± 0.15) times the atomic cross section σ_A in the energy range 110–250 KeV. This contradicts the conclusions of the theoretical work of Tuan and Gerjuoy⁴ for $E < 400$ KeV. Recent calculations of Ray and Saha⁵ on the ground-state capture of an electron from molecular hydrogen shows that $\sigma_M = 2\sigma_A$ at no energy and their calculated σ_M is in close agreement with the experiment.³ There has, however, been no theoretical calculations (to our knowledge) for the capture of electrons into excited states of the formed hydrogen atom in the process



The purpose of the present investigation is to study the nature of the charge-transfer cross section for capture of an electron into any excited state of the formed hydrogen atom. In particular, we are interested in (i) checking whether a hydrogen molecule may be considered as two independent hydrogen atoms for excited-state capture and (ii) the behavior of the total cross section σ_M as the principal quantum number n of the formed atom increases including the asymptotic case ($n \rightarrow \infty$).

Since our problem involves a many-body system, we cannot expect an exact solution of the relevant Schrodinger equation. We have thus used the first Born approximation (FBA) to study this problem.⁶ For rearrangement collisions, whether the FBA appropriates the exact situation or not is indeed related to the convergence question. Furthermore, it has been well known⁷ for a long time in the context of proton-hydrogen-atom charge transfer that neither the Brinkman-Kramers approximation using only the electron-nuclear interaction nor the Jackson-Schiff approximation using both the electron-nuclear and nuclear-nuclear interactions is correct. The main failings result from (i) the nonorthogonality of the initial and final wave functions and (ii) the nonphysical inclusion of nuclear-nuclear interaction by Jackson and Schiff in the transition matrix element when such a term should not influence the probability of charge transfer. In the absence of any other calculations for the charge-transfer process $H^+ + H_2 \rightarrow H(nlm) + H_2^+$, the FBA

with all its limitations, however, does provide useful estimates of cross sections possessing the correct general characteristics.

The outline of the present paper is as follows: In Sec. II, we derive the charge-exchange amplitudes using a contour integral representation of the wave function of the formed hydrogen atom. In Sec. III, we discuss the asymptotic nature of the transition amplitude as $n \rightarrow \infty$. Section IV is devoted to the discussion of our numerical results, while Sec. V gives concluding remarks.

II. THEORY

A. Formulation

The Schrodinger equation for rearrangement collisions of the proton-hydrogen-molecule system may be written as (atomic units are used unless otherwise stated)

$$\left(H_M - \frac{1}{2\mu_i} \nabla_{R_1}^2 + V_i\right)\psi = \left(H_I + H_A - \frac{1}{2\mu_f} \nabla_{R_2}^2 + V_f\right)\psi = E\psi, \quad (1)$$

where H_M , H_I , and H_A are the Hamiltonians for H_2 , H_2^+ , and H respectively; V_i is the prior interaction and V_f the post interaction.

The coordinates of this system are shown in Fig. 1, where the numbers 1 and 2 represent the two electrons in H_2 with coordinates \vec{r}_1 and \vec{r}_2 , respectively, while A and B are the protons in the molecule separated by internuclear distance $\vec{\rho}$. C is the incident proton positioned at \vec{R}_1 relative to the center of mass of the molecule, while \vec{R}_2 gives the position of the center of mass of the formed hydrogen atom, relative to the center of mass of the H_2^+ ion. \vec{r}_3 is the position of electron 1 relative to C.

In referring to Fig. 1, V_i may be written as

$$V_i = V_{1C} + V_{AC} + V_{BC} + V_{2C}. \quad (2)$$

E in Eq. (1) is obtained from the energy conservation

$$E = k_i^2/2\mu_i + E_M = k_f^2/2\mu_f + E_I + E_A, \quad (3)$$

where E_M is the initial energy of the molecule,

$$\phi_M(\vec{r}_1, \vec{r}_2, \vec{\rho}) = N_M \{U_M(r_1)U_M(r_2) + U_M(|\vec{r}_2 - \vec{\rho}|)U_M(|\vec{r}_1 + \vec{\rho}|) + c[U_M(r_1)U_M(|\vec{r}_2 - \vec{\rho}|) + U_M(r_2)U_M(|\vec{r}_1 + \vec{\rho}|)]\}, \quad (6)$$

where $U_M(r) = (Z_M^3/\pi)^{1/2} \exp(-Z_M r)$ and N_M is the normalization factor given by

$$N_M = 1/\{2[(1+c^2)(1+\Delta_M^2) + 4c\Delta_M]\}^{1/2},$$

$$\Delta_M = (1+Z_M\rho + \frac{1}{3}Z_M^2\rho^2) \exp(-Z_M\rho).$$

The values of c and Z_M depend on the choice of

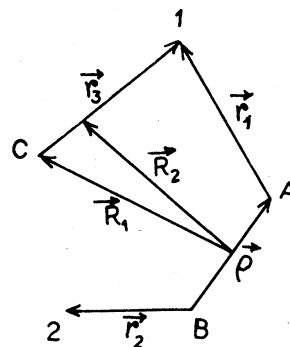


FIG. 1. Coordinate system for the H^+-H_2 collision. The letters represent the three protons, while the numbers stand for the electrons.

E_I the energy of H_2^+ and E_A the energy of the formed hydrogen atom. k_i and k_f are the momenta in the initial and final state, respectively. If the projectile proton is highly energetic, we may neglect the motion of the nuclear protons and thus we may consider them to be infinitely massive. In that case the initial reduced mass μ_i and final reduced mass μ_f will be given by

$$\mu_i = M, \quad \mu_f = M + 1,$$

where M is the proton mass in atomic units.

Solving Eq. (1), the differential cross section for electron capture, averaged over all orientations of the internuclear axis $\vec{\rho}$ of the hydrogen molecule is given in the FBA by

$$\frac{d\sigma_M}{d\Omega} = 2 \left(\frac{\mu_i \mu_f}{4\pi^2} \frac{k_f}{k_i} \right) \frac{1}{4\pi} \int \left| \langle \psi_f | V_i | \psi_i \rangle \right|^2 d\Omega_\rho. \quad (4)$$

The factor of 2 in the right-hand side of Eq. (4) occurs because either of the two molecular electrons may be involved in the capture process. The initial and final states are given by

$$\psi_i = e^{i\vec{k}_i \cdot \vec{R}_1} \phi_M(\vec{r}_1, \vec{r}_2, \vec{\rho}), \quad (5)$$

$$\psi_f = e^{i\vec{k}_f \cdot \vec{R}_2} \phi_I(\vec{r}_2, \vec{\rho}) U_{nlm}(\vec{r}_3),$$

where ϕ_M , ϕ_I , and U_{nlm} are the wave functions for H_2 , H_2^+ , and H, respectively. For the molecular wave function we take

wave function; for the Wang⁸ wave function $c=0$ and $Z_M=1.166$; for the Weinbaum⁹ wave function $c=0.256$ and $Z_M=1.193$. The H_2^+ wave function is given by

$$\phi_I(\vec{r}_2, \vec{\rho}) = N_I^\dagger [U_I(|\vec{r}_2 - \vec{\rho}|) \pm U_I(r_2)], \quad (7)$$

where

$$U_I(r) = (Z_I^3/\pi)^{1/2} \exp(-Z_I r),$$

$$N_I^\pm(r) = 1/[2(1 \pm \Delta_I)]^{1/2},$$

$$\Delta_I = (1 + Z_I \rho + \frac{1}{3} Z_I^2 \rho^2) \exp(-Z_I \rho).$$

Z_I is the effective charge of the molecular ion. The plus sign in the superscript of N_I refers to the gerade state of H_2^+ , while the minus sign refers to its ungerade state.

Using the wave functions given by Eqs. (6) and (7) and the interaction V_i given by Eq. (2), the capture amplitude for a particular orientation of the molecule may be expressed as^{4,5}

$$\langle \psi_f | V_i | \psi_i \rangle = I_1 + I_2 + I_3 + I_4, \quad (8)$$

where

$$I_1 = R_A^\pm R_B^\pm I_{ntm}, \quad (9)$$

$$I_2 = R_A^\pm R_B^\pm J_{ntm}, \quad (10)$$

$$I_3 = R_B^\pm [L(\vec{\beta}) \pm L(-\vec{\beta})], \quad (11)$$

$$I_4 = N_I^\pm N_M [J(\vec{\beta}) \pm J(-\vec{\beta})], \quad (12)$$

$$R_A^\pm = e^{i\vec{\alpha} \cdot \vec{\rho}/2} \pm e^{-i\vec{\alpha} \cdot \vec{\rho}/2}, \quad (13)$$

$$R_B^\pm = N_I^\pm N_M [(1 \pm c)\Delta_{IM} + (c \pm 1)\chi_{IM}(\rho)], \quad (14)$$

$$I_{ntm} = - \int f(\vec{r}_1, \vec{r}_3) \frac{1}{r_3} d\vec{r}_1 d\vec{r}_3, \quad (15)$$

$$J_{ntm} = \int f(\vec{r}_1, \vec{r}_3) \frac{1}{|\vec{r}_1 - \vec{r}_3|} d\vec{r}_1 d\vec{r}_3, \quad (16)$$

$$f(\vec{r}_1, \vec{r}_3) = \exp[i(-\vec{\alpha} \cdot \vec{r}_1 + \vec{\beta} \cdot \vec{r}_3)] U_{ntm}^*(r_3) U_M(r_1), \quad (17)$$

$$L(\vec{\beta}) = e^{i\vec{\alpha} \cdot \vec{\rho}/2} \int f(\vec{r}_1, \vec{r}_3) \frac{1}{|\vec{r}_1 - \vec{r}_3 - \vec{\rho}|} d\vec{r}_1 d\vec{r}_3,$$

$$J(\vec{\beta}) = e^{-i\vec{\alpha} \cdot \vec{\rho}/2} \int f(\vec{r}_1, \vec{r}_3) g(\vec{r}_1, \vec{r}_3, \vec{\rho}) d\vec{r}_1 d\vec{r}_3,$$

$$g(\vec{r}_1, \vec{r}_3, \vec{\rho}) = - \int d\vec{r}_2 [U_I(\vec{r}_2) \pm U_I(\vec{r}_2 + \vec{\rho})] \times \frac{1}{|\vec{r}_1 - \vec{r}_2 - \vec{r}_3|} [U_M(\vec{r}_2 + \vec{\rho}) + c U_M(\vec{r}_2)],$$

$$\vec{\alpha} = \vec{k}_f - \vec{k}_i,$$

$$\vec{\beta} = \frac{M}{M+1} \vec{k}_f - \vec{k}_i,$$

$$\Delta_{IM} = 8(Z_I Z_M)^{3/2} / (Z_I + Z_M)^3,$$

$$\chi_{IM}(\rho) = \frac{8(Z_I Z_M)^3}{\rho v^3} [Z_I(\rho v - 4Z_M)e^{-Z_M \rho} + Z_M(\rho v + 4Z_I)e^{-Z_I \rho}],$$

$$v = Z_I^2 - Z_M^2.$$

Again, the plus sign in the superscripts of R_A and R_B refers to the gerade transition, while the minus sign refers to the ungerade transition. The first term I_1 on the right-hand side of Eq. (8) arises due to the capture of electron 1 by virtue of the interaction V_{1C} between the electron 1 and the incident proton C . Thus I_1 may be called the molecular Brinkman-Kramers (MBK) amplitude in analogy with the atomic case. The proton-proton interactions ($V_{AC} + V_{BC}$) give rise to two terms I_2 and I_3 . Though it is not strictly possible to identify which proton binds electron 1, roughly we may think of I_2 as arising due to the interaction between the incident proton and the proton to which the electron 1 is bound. ($I_1 + I_2$), therefore, may be interpreted as the molecular Jackson-Schiff (MJS) amplitude in analogy with the atomic JS (Jackson-Schiff) matrix elements.

The third and the fourth terms I_3 and I_4 together may be thought of as representing capture of electron 1 from one of the atoms as a result of the interaction between the incoming proton and the other atom. The integrals involved in I_3 and I_4 are very difficult to compute. Moreover, these terms do not have any analog in the atomic case. We have therefore neglected these terms, hoping of course that their contributions would be insignificant compared to those of the other terms.

The molecular Brinkman-Kramers differential cross section $d\sigma_{\text{MBK}}/d\Omega$ and the molecular Jackson-Schiff differential cross section $d\sigma_{\text{MJS}}/d\Omega$ can then be obtained from Eq. (4) on replacing $\langle \psi_f | V_i | \psi_i \rangle$ by I_1 and $(I_1 + I_2)$, respectively. Thus

$$\frac{d\sigma_{\text{MBK}}}{d\Omega} = R_C^\pm |I_{ntm}|^2, \quad (18)$$

$$\frac{d\sigma_{\text{MJS}}}{d\Omega} = R_C^\pm |I_{ntm} + J_{ntm}|^2, \quad (19)$$

where

$$R_C^\pm = \frac{\mu_i \mu_f}{\pi^2} \frac{k_f}{k_i} (R_B^\pm)^2 [1 \pm j_0(\alpha \rho)] \quad (20)$$

with R_C^+ denoting gerade transition and R_C^- ungerade transition of the molecular ion.

B. Evaluation of the integrals I_{ntm} and J_{ntm}

For evaluation of these integrals we use a contour integral representation of the Laguerre polynomial and write the hydrogenic wave function as

$$U_{ntm}(\vec{r}) = N_{ntm} r^l P_l^m(\cos\theta) e^{im\phi} \frac{1}{2\pi i} \times \oint_{C_1} e^{-\gamma \alpha r} \frac{(x+1)^{n+l}}{(x-1)^{n-l}} dx, \quad (21)$$

where the contour C_1 includes the point $x=1$. The normalization constant N_{ntm} is given by

$$N_{nlm} = \left(\frac{\gamma_n^{2l+3} (n-l-1)!}{2^{2l} n(n+l)!} \frac{2l+1}{4\pi} \frac{(l-m)!}{(l+m)!} \right)^{1/2},$$

with

$$\gamma_n = 1/n, \quad \gamma_\alpha = \gamma_n x.$$

With this representation of $U_{nlm}(r)$, I_{nlm} , and J_{nlm} given by Eqs. (15) and (16) may be expressed as

$$I_{nlm} = -\frac{N_{nlm}}{2\pi i} \left(\frac{Z_M^3}{\pi} \right)^{1/2} \oint_{C_1} dx \frac{(x+1)^{n+l}}{(x-1)^{n-l}} \times \int \frac{F_{lm}(\vec{r}_1, \vec{r}_3)}{r_3} d\vec{r}_1 d\vec{r}_3, \quad (22)$$

$$J_{nlm} = -\frac{N_{nlm}}{2\pi i} \left(\frac{Z_M^3}{\pi} \right)^{1/2} \oint_{C_1} dx \frac{(x+1)^{n+l}}{(x-1)^{n-l}} \times \int \frac{F_{lm}(\vec{r}_1, \vec{r}_3)}{|\vec{r}_1 - \vec{r}_3|} d\vec{r}_1 d\vec{r}_3, \quad (23)$$

where

$$F_{lm}(\vec{r}_1, \vec{r}_3) = \exp(-i\vec{\alpha} \cdot \vec{r}_1 + i\vec{\beta} \cdot \vec{r}_3 - Z_M r_1 - \gamma_\alpha r_3) \times r_3^l P_l^m(\cos\theta_3) e^{im\phi_3}.$$

In this paper we concentrate on the study of the ns -state captures only. For this case we have

$l=m=0$. Taking the Fourier transforms of $\exp(-Z_M r_1)$ and $\exp(-\gamma_\alpha r_3)/r_3$, I_{n00} may be expressed as

$$I_{n00} = 16i N_{n00} Z_M (\pi Z_M^3)^{1/2} \frac{1}{(\alpha^2 + Z_M^2)^2} \times \oint_{C_1} dx \left(\frac{x+1}{x-1} \right)^n \frac{1}{\beta^2 + \gamma_n^2 x^2}. \quad (24)$$

The integrand contains three singularities—two simple poles at $x = \pm i\beta/\gamma_n$ and a pole of order n at $x=1$. We note, however, that the contour C_1 encloses only the singularity at $x=1$. The integral may therefore be easily evaluated by taking an infinitely large contour enclosing all the three singularities and applying the residue theorem. The result is

$$I_{n00} = -\frac{16\pi (Z_M^3 \gamma_n^3)^{1/2}}{(\alpha^2 + Z_M^2)^2} \frac{\sin n\theta}{\beta}, \quad (25)$$

where

$$\tan\theta = 2\beta\gamma_n/(\beta^2 - \gamma_n^2). \quad (26)$$

For the evaluation of J_{n00} , we again take the Fourier transforms of $\exp(-Z_M r_1)$, $\exp(-\gamma_\alpha r_3)$, and $1/|\vec{r}_1 - \vec{r}_3|$. Thus

$$J_{n00} = \frac{2(\gamma_n^3 Z_M^3)^{1/2}}{\pi^2 n i} \frac{\partial}{\partial Z_M} \oint_{C_1} dx \left(\frac{x+1}{x-1} \right)^n \frac{\partial}{\partial \gamma_\alpha} \int \frac{d\vec{s}}{s^2 [(\vec{\alpha} - \vec{s})^2 + Z_M^2] [\beta^2 - \vec{s}^2 + \gamma_\alpha^2]}. \quad (27)$$

The three-dimensional integral over \vec{s} may be done analytically by the Lewis¹⁰ method. But then we will be left with a contour integral which is difficult to handle numerically. On the other hand if this three-dimensional integral is reduced to a one-dimensional integral according to the prescriptions of Lewis, the contour integral can easily be evaluated. Following the latter procedure we get,

$$J_{n00} = \frac{8}{\gamma_n i} (\gamma_n^3 Z_M^3)^{1/2} \frac{\partial}{\partial Z_M} \int_0^\infty dy \oint_{C_1} dx \frac{(x+1)^{n-1}}{(x-1)^{n+1}} \frac{1}{E\gamma_\alpha^2 + 2F\gamma_\alpha + G}, \quad (28a)$$

where

$$\begin{aligned} E &= Dy^2 + 2Z_M y + 1, \\ F &= Dy(Z_M y + 1), \\ G &= Dy^2 [(\vec{\alpha} - \vec{\beta})^2 + Z_M^2] + \beta^2 [2Z_M y + 1], \\ D &= \alpha^2 + Z_M^2. \end{aligned} \quad (28b)$$

The integrand contains three singularities—a pole of order n at $x=1$ and two simple poles at

$$x = (1/\gamma_n E) [-F \pm i(GE - F^2)^{1/2}].$$

The contour C_1 , however, encloses only the singularity at $x=1$. In order to evaluate the integral over the contour C_1 , we again take an infinitely large circle enclosing all the singularities. Employing the residue theorem, we get after a

little algebra,

$$J_{n00} = -16\pi (\gamma_n^3 Z_M^3)^{1/2} \frac{\partial}{\partial Z_M} \int_0^\infty \frac{\text{Im}A}{B} dy, \quad (29)$$

where

$$A = (Z + \gamma_n)^{n-1} / (Z - \gamma_n)^{n+1}, \quad B = (GE - F^2)^{1/2},$$

$$Z = (-F + iB)/E.$$

III. ASYMPTOTIC FORM OF THE SCATTERING AMPLITUDES

In the case of atoms, the cross section for capture into the n th state is assumed to be proportional to n^{-3} . This behavior, however, is evident only for large quantum number n and very high

incident energy. Let us, therefore, study the behavior of the cross sections for excited-state capture from the molecule. As n tends to infinity, $\gamma_n = 1/n$ tends to zero. Hence Eq. (26) gives

$$\tan\theta = 2\gamma_n/\beta.$$

Since γ_n is very small, $\theta \approx 2\gamma_n/\beta$. Equation (25), therefore, reduces to

$$\lim_{n \rightarrow \infty} n^{3/2} I_{n00} = \frac{-16\pi(Z_M^5)^{1/2}}{(a^2 + Z_M^2)^2} \sin\left(\frac{2}{\beta}\right). \quad (30)$$

For the behavior of J_{n00} , we note that

$$\lim_{n \rightarrow \infty} A = \lim_{n \rightarrow \infty} \frac{(Z + \gamma_n)^{n+1}}{(Z - \gamma_n)^{n-1}} = e^{2/Z}.$$

We have, therefore,

$$\lim_{n \rightarrow \infty} n^{3/2} J_{n00} = -16\pi\sqrt{Z_M^3} \frac{\partial}{\partial Z_M} \int_0^\infty \frac{\text{Im}A}{B} dy, \quad (31)$$

where, now, $A = \exp(2/Z)$ and B remains the same as before.

IV. RESULTS AND DISCUSSIONS

For calculations of the cross sections, the effective charge of the molecular ion H_2^+ has been taken to be $Z_i = 1.4$. A different value of Z_i , for example, $Z_i = 1.228$ did not alter the results significantly. For the wave function of the hydrogen molecule, we have taken $Z_M = 1.193$ and $c = 0.256$, although we have studied the effect of other wave functions on the cross sections. For example, the Wang wave function does not change the results for gerade transition significantly. This, however, affects the results in transitions to ungerade states of the molecular ion as we shall see in the discussion of integrated cross sections below.

A. Differential cross sections

Figure 2 shows the plot of n -cubed differential cross sections (DCS) versus scattering angle θ (multiplied by M/m) for both the gerade and ungerade transitions of H_2^+ at the impact energy $E = 100$ keV for $n \rightarrow \infty$. The MBK DCS for both the gerade and ungerade transitions decrease monotonically from a peak in the forward direction with the increase of scattering angle θ , although the ungerade DCS is at least an order of magnitude less than that for the gerade transition throughout the angular range considered. The MJS cross sections on the other hand, fall off very rapidly from the peak value in the forward direction and becomes zero at $M\theta/m \approx 0.75$. These MJS curves again rise to a maximum and then fall off smoothly. The MBK peaks in the

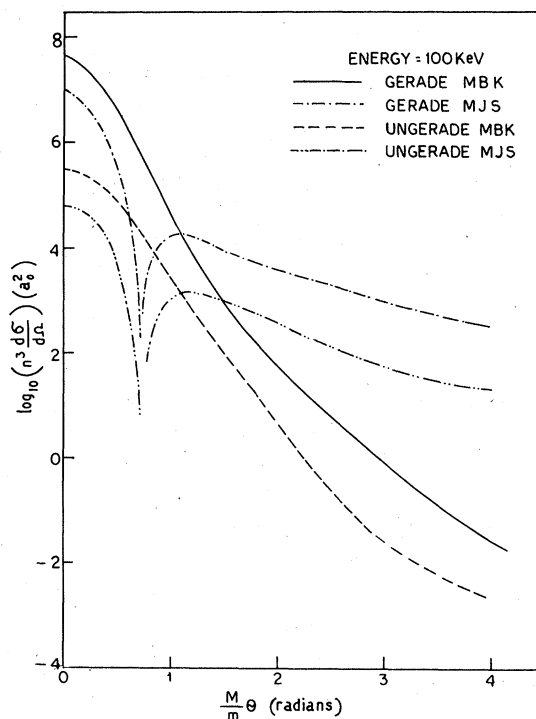


FIG. 2. n -cubed differential cross sections (in units of a_0^2) for both gerade and ungerade transitions of H_2^+ for $n \rightarrow \infty$ at the impact energy $E = 100$ keV.

forward direction are always higher than the corresponding MJS peaks. The zero in the MJS cross sections occurs because of the cancellation of the contributions arising from the electron-proton and proton-proton interactions and as expected from Eqs. (18) and (19) this occurs at the same value of the scattering angle for both the gerade and ungerade transitions. The zero has also been noticed in the FBA calculations of charge transfer from atomic hydrogen by proton impact.¹¹ It may be noted, however, that the occurrence of zero in the DCS is a result of the first-order theory for it is found in the atomic case that the zero disappears to varying degrees when approximations of higher order in one interaction or the other are employed.¹² We must point out here though, that we have treated the charge transfer from the molecule analogous to that from atom and neglected certain matrix elements as discussed in Sec. II. It is not easy to see if the DCS would vanish at the same value of θ or would vanish at all had we included those terms.

Figure 3 displays the n -cubed DCS for the incident energy 500 keV. In this case we also find the same features of the DCS as noted above except for the fact that the forward peaks have become sharper and the position of the zero in the DCS

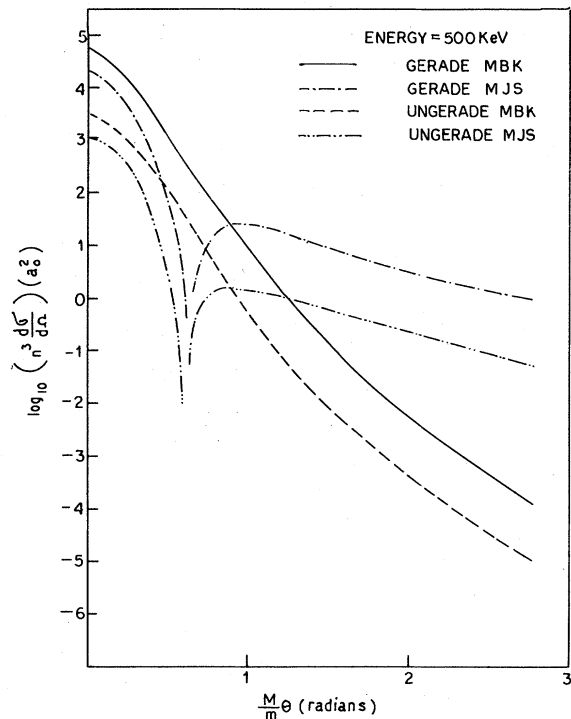


FIG. 3. Same as in Fig. 2 except that the impact energy $E = 500$ keV.

shifts towards the forward direction ($M\theta/m \approx 0.63$). For still higher energies we note the same features, namely, the forward peaks become sharper and the zero shifts towards $\theta = 0$. The major contribution to the total cross sections comes from the range $\theta = 0$ to the value of θ where the DCS becomes zero.

The n -cubed DCS for other excited s states, i.e., for finite n shows similar behavior. As a matter of fact, the differential cross sections for different n differ so little amongst themselves that they are almost coincident with the DCS of Figs. 2 and 3, although the total n -cubed cross sections are found to differ slightly, particularly for low n values.

B. Integrated cross sections

We denote the total MBK and MJS cross sections for the gerade transitions of H_2^+ by σ_{MBK}^g and σ_{MJS}^g , respectively, while those for the ungerade transitions are denoted by σ_{MBK}^u and σ_{MJS}^u , respectively. Those cross sections are obtained by integrating Eqs. (18) and (19) over the scattering solid angle. As it happens in all ion-atom collisions at high energies and as we have already noted, the major contribution to the total cross section comes from very near the forward direction. Thus, in order to facilitate integration over a very small angular

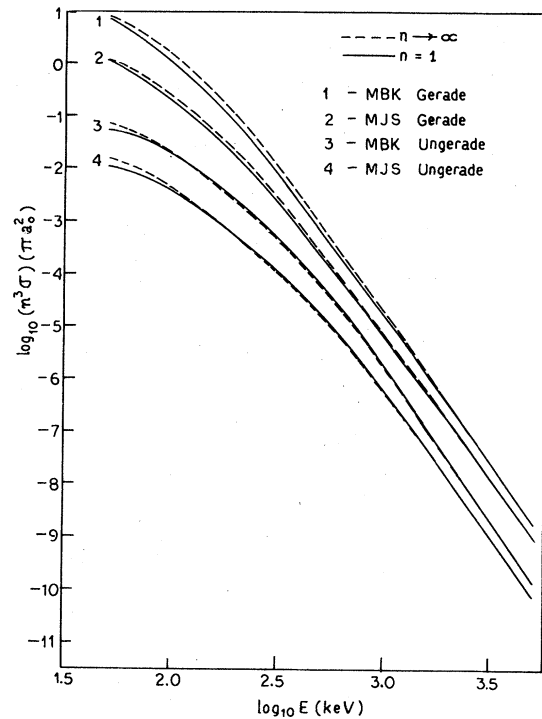


FIG. 4. n -cubed total cross sections in units of πa_0^2 as functions of impact energy E in keV.

range by Gaussian quadrature method, we use t instead of the scattering angle θ_s as our integration variable, where

$$\cos \theta_s = 1 - \frac{1}{k_i^2} \left(\frac{1+t}{1-t} \right),$$

k_i being the incident momentum. The convergence of the results has been tested by increasing the number of Gaussian points.

We have calculated σ_{MBK}^g , σ_{MJS}^g , σ_{MBK}^u , and σ_{MJS}^u for capture into a number of excited s states of the formed hydrogen atom at different energies in the range 50 keV to 5 MeV. For all finite n values the cross sections are calculated with the use of Eqs. (25) and (29), whereas for the asymptotic cross sections ($n \rightarrow \infty$), the limiting expressions as given by Eqs. (30) and (31) have been employed. Figure 4 shows the behavior of the asymptotic cross sections ($n \rightarrow \infty$), where we have also displayed the cross sections for ground-state capture from our earlier calculations⁵ for comparison. To get an idea about the behavior of cross sections for low and intermediate n , we record the cross sections for $n = 2, 8, 16$, and ∞ in Table I. It is easy to find from this table that with the increase of n , the n -cubed cross sections for excited-state capture tend to a constant in a regular manner at each incident energy. The n -cubed cross sections for $n = 16$, for example, are quite close to the cor-

TABLE I. The total n -cubed cross sections (in πa_0^2) for both the gerade and ungerade transitions of H_2^+ . The notation $a(-b)$ implies $a \times 10^{-b}$.

E (keV)	$n \rightarrow$	σ^g				σ^u			
		2	8	16	∞	2	8	16	∞
50	MBK	8.79	8.87	8.87	8.87	5.61(-2)	5.08(-2)	5.05(-2)	5.05(-2)
	MJS	1.18	1.20	1.20	1.20	1.15(-2)	1.03(-2)	1.02(-2)	1.02(-2)
100	MBK	1.33	1.45	1.46	1.46	1.71(-2)	1.70(-2)	1.69(-2)	1.69(-2)
	MJS	2.15(-1)	2.28(-1)	2.28(-1)	2.28(-1)	3.27(-3)	3.19(-3)	3.18(-3)	3.18(-3)
200	MBK	8.84(-2)	9.70(-2)	9.74(-2)	9.75(-2)	2.49(-3)	2.58(-3)	2.59(-3)	2.59(-3)
	MJS	1.91(-2)	2.05(-2)	2.05(-2)	2.05(-2)	5.35(-4)	5.44(-4)	5.44(-4)	5.44(-4)
500	MBK	8.21(-4)	8.70(-4)	8.72(-4)	8.72(-4)	6.18(-5)	6.43(-5)	6.44(-5)	6.44(-5)
	MJS	2.58(-4)	2.70(-4)	2.71(-4)	2.71(-4)	1.84(-5)	1.89(-5)	1.90(-5)	1.90(-5)
1000	MBK	1.76(-5)	1.81(-5)	1.81(-5)	1.81(-5)	1.73(-6)	1.77(-6)	1.78(-6)	1.78(-6)
	MJS	6.58(-6)	6.72(-6)	6.73(-6)	6.73(-6)	6.57(-7)	6.73(-7)	6.73(-7)	6.73(-7)
2000	MBK	4.55(-7)	4.61(-7)	4.61(-7)	4.61(-7)	2.75(-8)	2.80(-8)	2.80(-8)	2.80(-8)
	MJS	2.01(-7)	2.03(-7)	2.03(-7)	2.03(-7)	1.23(-8)	1.25(-8)	1.25(-8)	1.25(-8)
5000	MBK	1.93(-9)	1.95(-9)	1.95(-9)	1.95(-9)	1.47(-10)	1.48(-10)	1.48(-10)	1.48(-10)
	MJS	9.97(-9)	1.00(-9)	1.00(-9)	1.00(-9)	7.65(-11)	7.69(-11)	7.69(-11)	7.69(-11)

responding asymptotic values ($n \rightarrow \infty$) at all energies. Thus the n^{-3} law for the total-capture cross sections is satisfied throughout the energy range considered. Experiments on the excited-state captures in the high-energy region are, to our knowledge, very rare; although there have been some experiments in the low-energy region. For instance, there are the data of Hughes et al.¹³ on 3s and 4s captures in the energy range 5–120 keV and that of Bayfield¹⁴ on 2s capture in the energy range 2–70 keV. The agreement between the FBA and experiments can not be expected to be good in the low-energy region. Thus we note, for example, that the experimentally determined¹⁴ $n^3\sigma(1s-2s)$ at 50 keV is (1.6376 ± 0.1728) , whereas our calculated $n^3\sigma_{MJS}^g(1s-2s)$ is 1.1807.

In order to test whether a hydrogen molecule may be considered as a pair of independent hydrogen atoms for purposes of charge transfer, we have calculated the cross-section ratios

$$R_1 = \sigma_{MBK}^g(1s-ns)/2\sigma_{ABK}(1s-ns)$$

and

$$R_2 = \sigma_{MJS}^g(1s-ns)/2\sigma_{AJS}(1s-ns), \quad (32)$$

where the values of the atomic BK and JS cross sections $\sigma_{ABK}(1s-ns)$ and $\sigma_{AJS}(1s-ns)$ have been taken from Sil et al.¹¹. Figure 5 shows R_1 and R_2 for 2s capture. The variation of R_1 and R_2 with energy is due to interference between the two-capture amplitudes from the two atomic centers in the molecule. It is also seen that none of these ratios R_1 and R_2 is unity, as one would expect if the hydrogen molecule were to be treated as a pair of independent hydrogen atoms. Similar behavior is noted for other s-state captures. Ryding

et al.¹⁵ performed an experiment on 2s capture in which they measured the cross-section ratio

$$Q_1 = \sigma_A(1s-2s)/\sigma_M(1s-2s),$$

where $\sigma_A(1s-2s)$ denotes the cross section for capture into 2s state from atomic hydrogen and

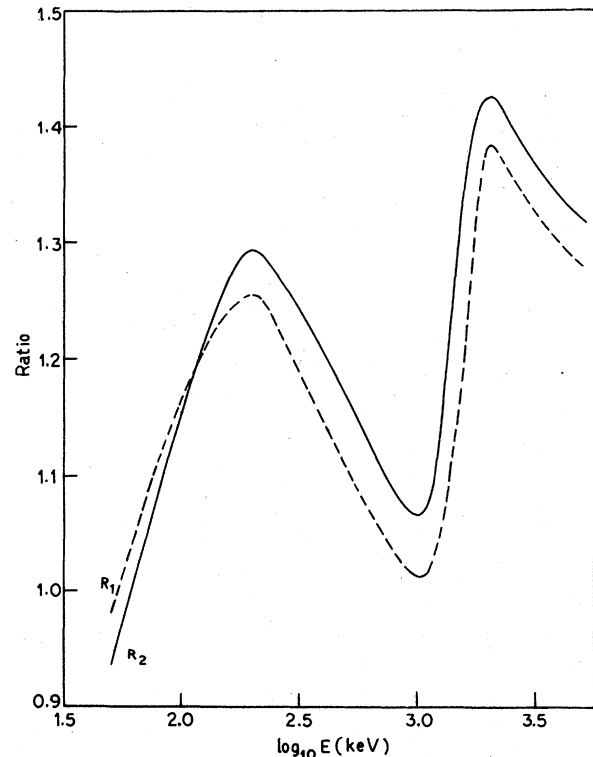


FIG. 5. Ratios R_1 and R_2 [see Eq. (32)] as functions of impact energy E in keV.

$\sigma_M(1s-2s)$ that from molecular hydrogen. Their measurement, however, was limited to the energy range 40–120 keV. The agreement between our calculated values of Q_1 and those of the experiment is quite good within the limits of experimental error. For example, at 50 keV, the experiment gives $Q_1 = (0.59 \pm 0.12)$, while our theoretical values are $Q_1^{\text{MJS}} = 0.534$ and $Q_1^{\text{MBK}} = 0.510$. At 100 keV, we have $Q_1^{\text{expt}} = (0.34 \pm 0.12)$, $Q_1^{\text{MJS}} = 0.434$, $Q_1^{\text{MBK}} = 0.429$. Thus a hydrogen molecule can not be regarded as a pair of independent atoms for purposes of charge transfer.

In order to assess the importance of ungerade transitions we look at the ratio $Q_2 = \sigma_{\text{MJS}}^u / \sigma_{\text{MJS}}^g$. Equation (19) gives

$$Q_2 = \frac{[(\Delta_{IM} - \chi_{IM})(1-c)]^2 (1 + \Delta_I)(a_1 - a_2)}{[(\Delta_{IM} + \chi_{IM})(1+c)]^2 (1 - \Delta_I)(a_1 + a_2)}$$

with

$$a_1 = \int |I_{n00} + J_{n00}|^2 d\Omega,$$

$$a_2 = \int |I_{n00} + J_{n00}|^2 j_0(\alpha\rho) d\Omega.$$

Because of the occurrence of $j_0(\alpha\rho)$ in the integrand, a_2 tends to zero in the high-energy limit. Thus the high-energy limit of the above ratio Q_2

is

$$Q_2(E \rightarrow \infty) = \left(\frac{(\Delta_{IM} - \chi_{IM})(1-c)}{(\Delta_{IM} + \chi_{IM})(1+c)} \right)^2 \frac{1 + \Delta_I}{1 - \Delta_I},$$

which is independent of energy E and principal quantum number n . It is obvious from above that one obtains the same high-energy limit for the ratio $\sigma_{\text{MBK}}^u / \sigma_{\text{MBK}}^g$. Since the major contribution to the total cross section comes from a very small angular range, $j_0(\alpha\rho)$ may be assumed to vary very slowly in the angular domain of interest and hence it may be taken outside the integral for a_2 . Thus the integral a_2 vanishes approximately at the zeros of $j_0(\alpha\rho)$. The ratio Q_2 , therefore, should oscillate about the high-energy value $Q_2(E \rightarrow \infty)$ with rapidly decreasing amplitude and finally attain the high-energy limit ratio. Figure 6 shows a plot of this ratio Q_2 against energy for ground state and 4s-state captures. Curves b and d are for ground-state captures calculated with Weinbaum and Wang wave function, respectively, while curves a (Weinbaum) and c (Wang) represent 4s-state capture. The straight lines I and II indicate the high energy-limit ratio for the Weinbaum and Wang wave functions, respectively. All these curves show the expected behavior except for the fact that Q_2 varies drastically with different types of mole-

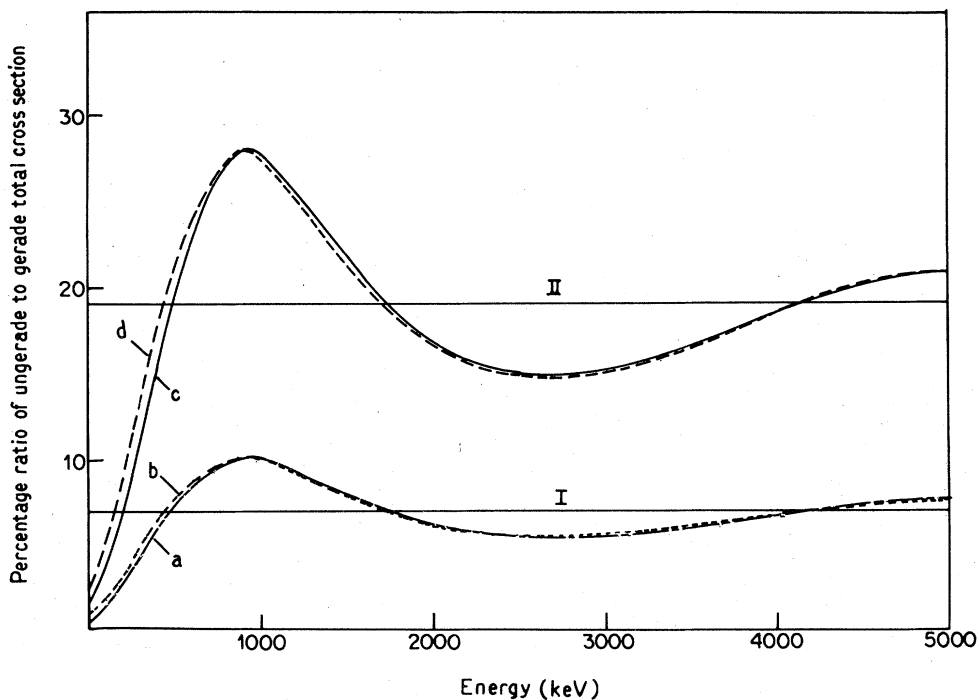


FIG. 6. The percentage ratio of ungerade to gerade total cross section. Curves b and d denote ground-state-capture cross-section ratios calculated with Weinbaum and Wang wave function, respectively, while curves a (Weinbaum) and c (Wang) represent the ratios for 4s-state capture. The straight lines I and II indicate the high-energy-limit ratio for the Weinbaum and Wang wave functions, respectively.

cular wave function. Starting from a low value in the low-energy region Q_2 reaches a peak—about 10% for the Weinbaum wave function and about 28% for the Wang wave function — at 900 keV. As the energy is increased further, Q_2 decreases and then rises again, characteristic of oscillation of $j_0(\alpha\rho)$ about the high-energy value $Q_2(E\rightarrow\infty)$ — about 19% for the Wang wave function and 7% for the Weinbaum. Physically, these peaks and dips in this ratio Q_2 are due to the constructive and destructive interference in the ungerade (and the corresponding destructive and constructive interference in the gerade) transitions. We also note that Q_2 for ground-state capture does not differ too much from that for the $4s$ -state capture in the case of Weinbaum wave function, although they differ a little in the case of Wang wave function, particularly in the low-energy region.

Since it is rather difficult to compute the Born cross section for excited-state capture, Bates and Dalgarno¹⁶ estimated the Born cross section for excited-state charge transfer from the hydrogen atom by assuming that

$$\frac{\sigma_{\text{AJS}}(1s-ns)}{\sigma_{\text{AJS}}(1s-1s)} = \frac{\sigma_{\text{ABK}}(1s-ns)}{\sigma_{\text{ABK}}(1s-1s)}.$$

Thus from a knowledge of both the ground state and ns -state atomic BK cross sections and the ground-state JS cross section, the ns -state atomic JS cross section $\sigma_{\text{AJS}}(1s-ns)$ may be evaluated. In order to see whether such estimation is possible in the case of charge transfer from molecule also, we have calculated the ratios

$$R_3 = \frac{\sigma_{\text{MBK}}(1s-ns)}{\sigma_{\text{MBK}}(1s-1s)}$$

and

$$R_4 = \frac{\sigma_{\text{MJS}}(1s-ns)}{\sigma_{\text{MJS}}(1s-1s)}$$

for both the gerade and ungerade transitions. We find that R_3 becomes approximately equal to R_4 as the impact energy increases. This conclusion is valid for any n . A better estimation of the MJS cross section $\sigma_{\text{MJS}}(1s-ns)$ is possible, however, even at low impact energies, if one assumes

$$\frac{\sigma_{\text{MJS}}(1s-ns)}{\sigma_{\text{MJS}}(1s-2s)} = \frac{\sigma_{\text{MBK}}(1s-ns)}{\sigma_{\text{MBK}}(1s-2s)}.$$

The energy dependence of the ratio $R_5 = \sigma_{\text{MJS}}/\sigma_{\text{MBK}}$ is similar to that found in the case of atoms.¹¹ For a given excited state, R_5 increases as the energy increases for both the gerade and ungerade transitions. Also, as the energy increases $R_5^g \approx R_5^u$ for any n . Furthermore R_5 is found to be approximately independent of n for any $n > 1$.

V. CONCLUDING REMARKS

To summarize, therefore, we have based our work on the molecular Brinkman-Kramers and molecular Jackson-Schiff amplitudes. Within the framework of these approximations, we have calculated the charge-transfer cross sections for proton-hydrogen-molecule collisions in which the hydrogen atom formed is in various excited s states including the asymptotic case ($n\rightarrow\infty$). In the case of excited-state formation of hydrogen atom also, a hydrogen molecule cannot be regarded as a pair of independent hydrogen atoms at any energy just as in the case of ground-state formation of hydrogen atoms. We also note that the charge-transfer cross sections satisfy inverse n^3 law for large n . In the energy range considered (50 keV–5 MeV), the charge transfer involving the gerade transitions of the molecular ion is the most important process, although depending on the choice of molecular wave function there is a 10–28% chance of the charge-transfer process involving the ungerade transition. As we have already pointed out in Sec. I, the Born matrix elements are evaluated using initial and final wave functions which are not orthogonal to each other. A proper calculation should take into account the effect of non-orthogonality of wave functions. Work along this line is in progress and will be reported later. From the work of Band,⁷ however, it appears that the main conclusions of this paper will remain valid even when the effect of nonorthogonality is taken into account, at least in the high-energy region.

ACKNOWLEDGMENT

We are indebted to Professor N. C. Sil for valuable discussions.

¹H. C. Brinkman and H. A. Kramers, Proc. Nat. Acad. Sci. (Amsterdam) **33**, 973 (1930); J. D. Jackson and H. Schiff, Phys. Rev. **89**, 359 (1953); R. A. Mapleton, *ibid.* **126**, 1477 (1962); K. Omidvar, *ibid.* **153**, 121 (1967); I. M. Cheshire, Proc. Phys. Soc. London **83**, 227 (1964).

²C. Barnett and H. K. Reynolds, Phys. Rev. **109**, 355 (1958); U. Schryber, Helv. Phys. Acta **39**, 562 (1966); J. F. Williams, Phys. Rev. **157**, 97 (1967); L. H. Touburen, M. Y. Nakai, and R. A. Langley, *ibid.* **171**, 355 (1968); H. Tawara and A. Russek, Rev. Mod. Phys. **45**, 178 (1973).

- ³A. B. Wittkower, G. Ryding, and H. B. Gilbody, Proc. Phys. Soc. London 89, 541 (1966).
- ⁴T. F. Tuan and E. Gerjuoy, Phys. Rev. 117, 756 (1960).
- ⁵P. P. Ray and B. C. Saha, Phys. Lett. A71, 415 (1979).
- ⁶For a brief account of this work, see P. P. Ray and B. C. Saha, in *Electronic and Atomic Collisions, Proceedings of the XIth ICPEAC Abstracts of Contributed papers*, edited by K. Takayanagi and N. Oda (The Society for Atomic Collision Research, Kyoto, 1979), p. 824.
- ⁷D. R. Bates, Proc. R. Soc. London Ser. A 247, 294 (1958); R. H. Bassel and E. Gerjuoy, Phys. Rev. 117, 749 (1960); Y. B. Band, Phys. Rev. A 8, 243 (1973).
- ⁸S. C. Wang, Phys. Rev. 31, 597 (1928).
- ⁹S. Weinbaum, J. Chem. Phys. 1, 593 (1933).
- ¹⁰R. R. Lewis, Jr., Phys. Rev. 102, 537 (1956).
- ¹¹N. C. Sil, B. C. Saha, H. P. Saha, and P. Mandal, Phys. Rev. A 19, 655 (1979).
- ¹²P. J. Kramer, Phys. Rev. A 6, 2125 (1972); C. S. Shastri, A. K. Rajagopal, and J. Callaway, *ibid.* 6, 268 (1972).
- ¹³R. H. Hughes, H. R. Dawson, and B. M. Doughty, Phys. Rev. 164, 166 (1967).
- ¹⁴J. E. Bayfield, Phys. Rev. 182, 115 (1969).
- ¹⁵G. Ryding, A. B. Wittkower, and H. B. Gilbody, Proc. Phys. Soc. London 89, 547 (1966).
- ¹⁶D. R. Bates and A. Dalgarno, Proc. Phys. Soc. London Ser. A 66, 972 (1953).